JMEPEG (2010) 19:52–58
DOI: 10.1007/s11665-009-9422-x

1059-9495/$19.00

Influence of In Situ Reaction on the Microstructure of SiC_p/AlSi7Mg Welded by Nd:YAG Laser with Ti Filler

Kelvii Wei Guo

(Submitted July 27, 2008; in revised form February 26, 2009)

The effect of in situ reaction on the microstructure of Nd:YAG laser welded joints of aluminum matrix composite SiC_p/AlSi7Mg was studied. Results showed that the laser welding with Ti filler improved the tensile strength of welded joints. Moreover, the laser welding with in situ reaction effectively restrained the pernicious Al_4C_3 forming reaction in the interface between aluminum matrix and reinforcement particles. Simultaneously, the reaction-formed TiC phase distributed uniformly in the weld. This permitted SiC_p/AlSi7Mg composite to be successfully welded by Nd:YAG laser.

Keywords AlSi7Mg, in situ reaction, Nd:YAG laser, Ti

1. Introduction

The high specific strength, good wear resistance, and corrosion resistance of aluminum matrix composites (AMCs) have led to a number of industrial applications (Ref 1-5). For example, AMCs are widely used in automobile, aerospace industries, structural components, and heat- and wear-resistant parts such as automotive brake discs. Owing to the typical characteristics of production methods, the distribution of the reinforcement in stir-cast AMCs is generally inhomogeneous (Ref 1, 5). Furthermore, the ceramic reinforcement may be in the form of particles, short fibres, or whiskers (Ref 5, 6). The discontinuous nature of the reinforcement creates several problems in imparting strength and quality to weld joints. Although there are several welding techniques currently available for joining AMCs (Ref 7-15), there still exist quality problems due to the factors elaborated later.

1.1 Distribution of Reinforcements in Weld

Normally, properties of welded joints are directly influenced by the distribution of reinforcement in the weld. When particle reinforcements are distributed uniformly in the weld, the tensile strength of welded joints is likely to reach 80% (or even slightly higher) of that of the parent AMCs (Ref 16, 17). When the particle reinforcements are either agglomerated or absent in the weld (Ref 18), the properties of welded joints degrade markedly, resulting in joint failure.

Kelvii Wei Guo, Department of Manufacturing Engineering and Engineering Management, City University of Hong Kong, 83 Tat Chee Avenue, Kowloon Tong, Kowloon, Hong Kong. Contact e-mail: kelviiguo@yahoo.com.

1.2 Interface Between Particle Reinforcements and Aluminum Matrix

The high welding temperature in fusion welding (typically, TIG, laser welding, electron beam, etc.) is likely to yield pernicious Al_4C_3 phase in the interface. Moreover, the long welding time (e.g. several days in certain occasions) needed in solid state welding methods (such as diffusion welding) normally leads to low efficiency and formation of harmful and brittle intermetallic compounds in the interface.

This work studies the technique of welding the stir-cast AMC SiC_p/AlSi7Mg by Nd:YAG laser with pure titanium as filler. This study has been specifically concerned with the in situ reinforcement effect of Ti on the microstructures of laser welded joints, which have been examined using scanning electron microscope (SEM), transmission electron microscope (TEM), and x-ray diffraction (XRD). The study aims at providing some ground work for further studies in this field.

2. Experimental Material and Process

2.1 Experimental Material

Stir-cast SiC_p/AlSi7Mg AMC, reinforced with 20% volume fraction SiC particle of 12 μm mean size, was used as the welding specimens. The tensile strength of the specimen was 240 MPa. Figure 1 shows the sample microstructure and Table 1 summarizes the chemical composition of the matrix alloy. Pure titanium was used as the filler metal.

2.2 Experimental Process

The stir-cast AMC specimens were individually wire-cut to $3 \times 10 \times 35$ mm^3 size. The quench-hardened layer induced by wire-cut and the oxide on the surfaces of specimens were removed by polishing on 400 # (35 μm in average) emery cloth. The pure titanium filler was then machined to 3×10 mm size with thicknesses of 0.15, 0.3, 0.45, 0.5, 0.6, and 0.75 mm, respectively. The composite specimens were ultrasonically cleaned in acetone at 28-34 Hz frequency for 5 min, then carefully pure ethyl alcohol rinsed and blow-dried before

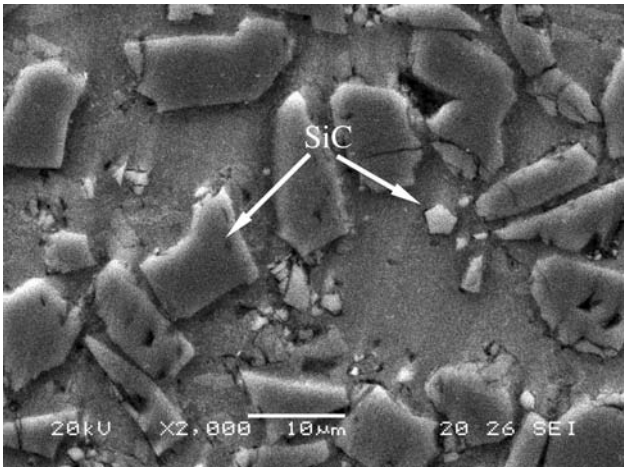

Fig. 1 Microstructure of SiC_p/AlSi7Mg aluminum matrix composite

Table 1 Composition of AlSi7Mg

Composition, wt.%			
Si	**Mg**	**Ti**	**Al**
6.5-7.5	0.3-0.5	0.08-0.2	Bal.

welding. The specimens were mounted into a clamping device on the platform of a GSI Lumonics Model JK702H Nd:YAG TEM_{00} mode laser system.

A repeated cleaning process was used for machined titanium, and then the titanium filler was carefully sandwiched between the two composite specimens in the clamp. Thereafter, specimens were welded immediately by the Nd:YAG laser with wavelength of 1.06 μm, defocused distance of 10 mm so as to give a focus spot diameter of approximately 1.26 mm, laser fluence energy 2 J, frequency 25 Hz, and pulse duration 4 ms. In welding, the relative speed of the laser and the welding pieces (i.e. feed rate) was set at 300 mm/min.

Tensile strength of the joint was measured on a MTS Alliance RT/30 electron-mechanical material testing machine with a straining velocity of 0.5 mm/min. The cross-section of welded joints was wire-cut for optical microscopy (OM), SEM, and TEM. SEM was used to analyze the microstructure at the weld joints and the fractured tensile test-pieces of the joints. Optical microscope was used for observing the structure of a large area. TEM and energy dispersive x-ray analysis (EDX) were used to analyze the interface between the newly formed phases and the matrix, the distribution of chemical elements and spectra at the joints. The Nd:YAG laser with similar setting conditions and feed rate was also used to weld the AMC specimens without filler.

3. Results and Discussion

3.1 Microstructures and Properties of Welded Joints

The microstructure (Fig. 2) of the traditional Nd:YAG laser weld without filler shows that there were lots of acicular Al_4C_3 particles in the weld, which led to a low joint tensile strength (Fig. 3) of 91 MPa (about 37.9% of parent AMC). The corresponding fracture surface is shown in Fig. 4. It shows some bare reinforcement particles (SiC) distributed on the fracture surface, suggesting that the reinforcement particles had not been perfectly wet and decreased the tensile strength of welded joints.

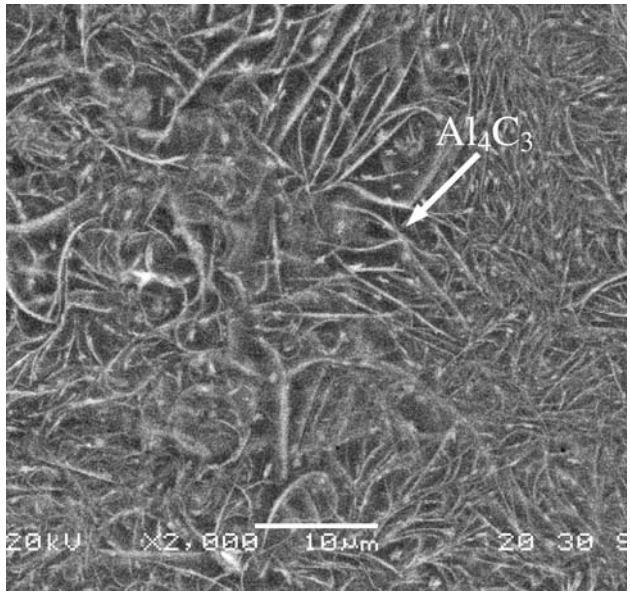

Fig. 2 Microstructure of the weld without Ti filler

The microstructure of the in situ reinforced AMC with 0.3 mm thick Ti filler is shown in Fig. 5. This figure shows a uniform distribution of in situ reinforcements, complete fusion and absence of Al_4C_3. These features resulted in higher tensile strength (Fig. 3) of the joint. The reinforcement particles are distributed more uniformly than in parent composite (cf. Fig. 1 and 5) and this improved the properties of welded joints as the newly formed in situ reinforcement particles (Fig. 5) replaced the initial reinforcement particles (Fig. 1). The dimples in the fracture surface (Fig. 6) suggest that (i) the newly formed reinforcement particles had been perfectly wet (Ref 19, 20) and (ii) the harmful composite structure of the initial welding viz. reinforcement/Ti/reinforcement had been changed to reinforcement/matrix/reinforcement. XRD pattern of the fracture surface (Fig. 7) of the weld joint did not reveal any harmful and brittle phases such as Al_4C_3. According to the intensity spectra shown in Fig. 7, the newly formed reinforcement particle in the weld was identified as TiC.

Figure 8 shows the macro-structure of welded joint with Ti filler. Basically, the weld consisted of three main areas, namely the in situ reinforcement area A, the two transitional areas B and C, and the reinforcement-denuded area D. Their individual microstructures are shown in Fig. 9. The microstructures indicated that the initial reinforcement SiC particles were completely replaced by the newly formed in situ reinforcement TiC particles that mainly resulted in the formation of the area A (Fig. 9a). In area B, the newly formed TiC particles and the SiC particles coexist (Fig. 9b). In area C, very little newly formed TiC particles were found (Fig. 9c). In area D, only SiC particles exist (Fig. 1). It was found that Al_4C_3 had been effectively

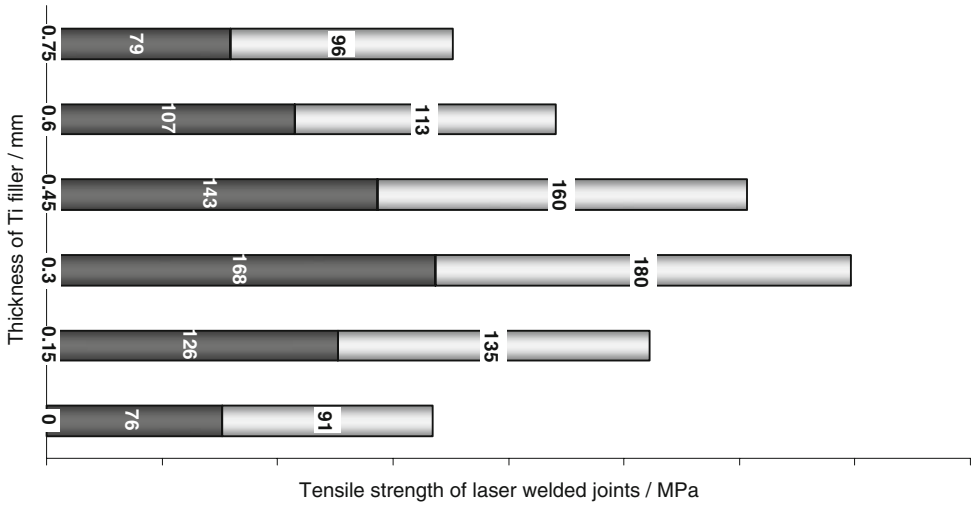

Fig. 3 Tensile strength of laser welded joints with various Ti filler thicknesses

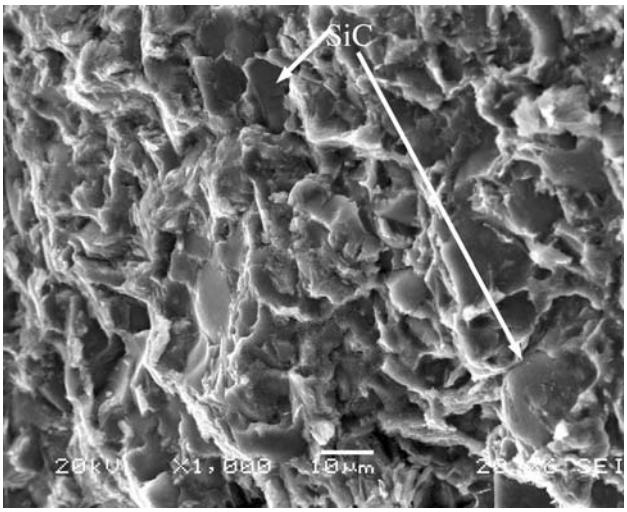

Fig. 4 Fractograph of the laser welded joint without Ti filler

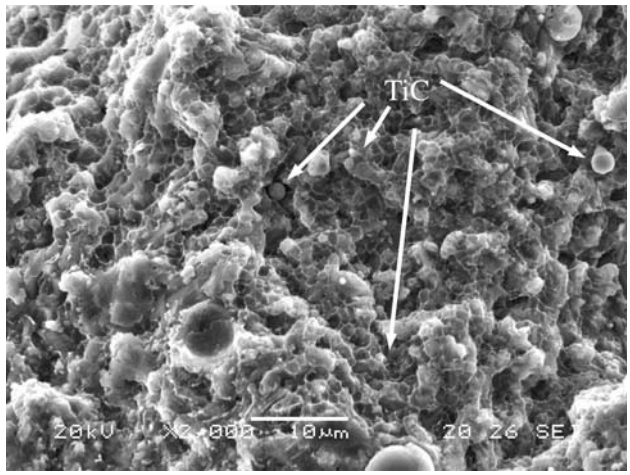

Fig. 6 Fractograph of the laser welded joint with 0.3 mm thick Ti filler

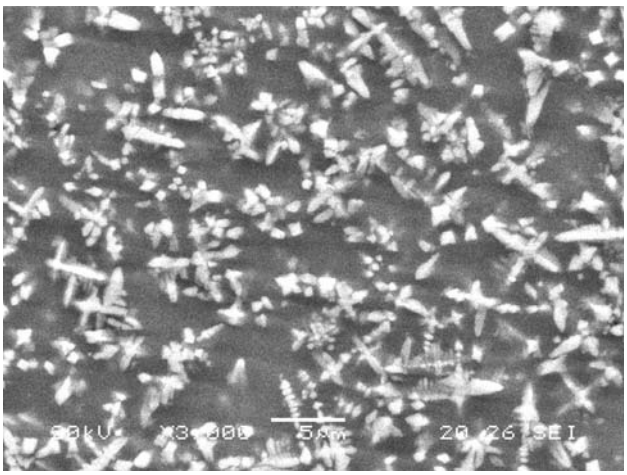

Fig. 5 Microstructure of in situ reinforcement by laser welding with 0.3 mm thick Ti filler

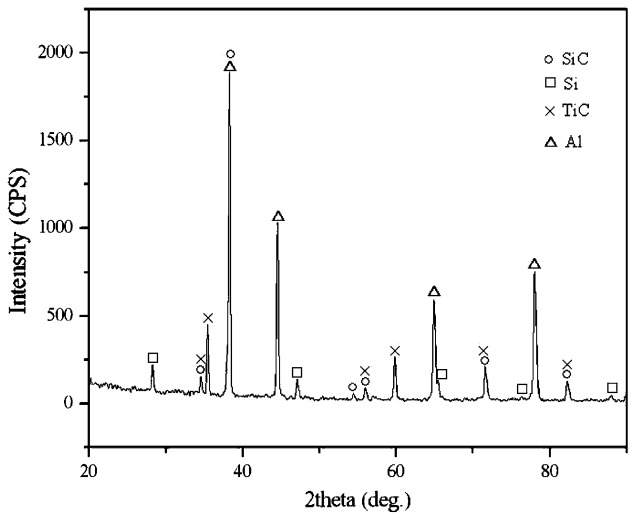

Fig. 7 XRD pattern of the fracture surface for laser welding with 0.3 mm thick Ti filler

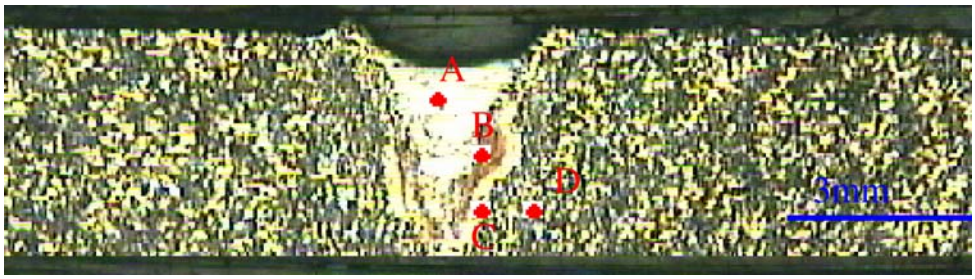

Fig. 8 Macro-structure of the laser welded joint with 0.3 mm thick Ti filler

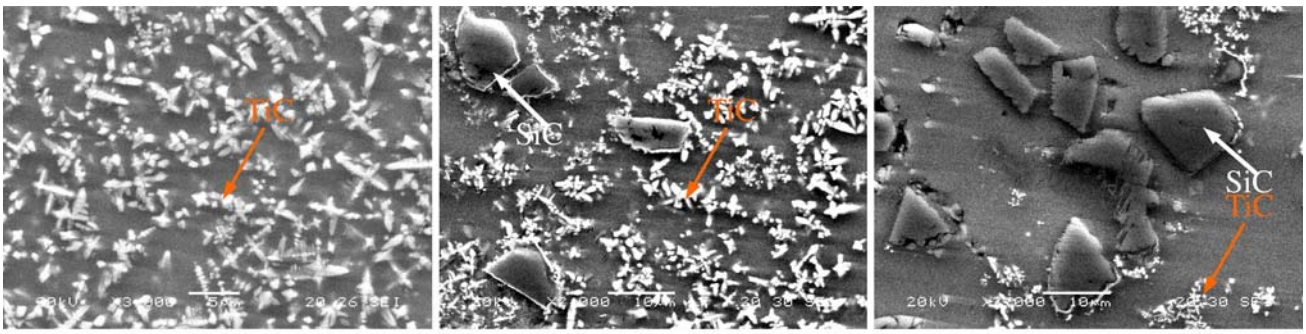

Fig. 9 Microstructures of the different areas in the laser weld with 0.3 mm thick Ti filler. (a) area A; (b) area B; (c) area C

eliminated in the welded area. Hence, the properties of the welded joints improved markedly and their achievable tensile strength was up to 180 MPa (Fig. 3) that was about 75% of the strength of SiC_p/AlSi7Mg.

3.2 Element Distribution in the Transition Area

Figure 10 illustrates the element distribution of the area B in the weld as shown in Fig. 8 and 9(b). It shows that the newly formed in situ reinforcement particles surrounded the SiC particles which offered a high density area for the nucleation of in situ TiC. During welding, due to the temperature gradient and surface tension in the weld pool, convection can occur. Moreover, under the effect of plasma, the weld pool would be stirred intensively. Consequently, the stirring effect in the weld pool by laser irradiation would promote the TiC formation (cf. Fig. 10b and c) by the following reaction:

$$\mathrm{Ti(l)} + \mathrm{SiC(s)} \rightarrow \mathrm{TiC(s)} + \mathrm{Si(s)}$$

The free energy required to form TiC is much lower than that for Al_4C_3 when the reaction temperature is above 800 °C (Ref 21-23). The affinity between Ti and C in the Nd:YAG laser welding was therefore greater than that of Al and C. The chemical reaction between Ti and SiC in the weld pool would take precedence over the reaction between Al and SiC and thus restrain the formation of the Al_4C_3. Furthermore, the Si formed during the reaction is distributed in the substrate under the stirring effect of weld pool.

3.3 Influence of Ti Filler Thickness

The microstructures of in situ reinforcement with various thicknesses (δ) of Ti filler are shown in Fig. 11 and the corresponding fractographs are shown in Fig. 12. The amount of the in situ formed TiC was distinctly increased with the increase in the thickness of Ti filler. Test indicated that maximum strength of welded joints (Fig. 5) was achieved at Ti filler thickness of 0.3 mm (Fig. 3 and 6). This was because the TiC particles were uniformly distributed in the weld and the initial irregular (mostly hexagonal shape, Fig. 1) reinforcement SiC particles in the weld were no longer observed (Fig. 5 and 6). Moreover, Al_4C_3 formation was restrained (Fig. 5 and 9a). At the thickness of Ti filler below 0.3 mm, due to the lack of titanium, TiC particles did not form sufficiently (Fig. 12a) and a number of Al_4C_3 particles formed in the weld. When the thickness of Ti filler was just beyond 0.3 mm, the properties of the joints tended to become poorer again (Fig. 12b). This was because the laser input energy melted the Ti filler; as a result, the substrate could not be melted efficiently to form the TiC and temperature of weld pool decreased to some extent. Therefore, the stirring effect in the weld pool decreased and resulted in coarse columnar crystals and fine equiaxed crystals (Fig. 12b). When the thickness of Ti filler was further increased (Fig. 12c), higher laser input energy was needed to melt the titanium. The temperature of weld pool decreased, the substrate did not melt, and the effective stirring effect between the titanium and substrate was restrained. Simultaneously, the percentage of liquid Ti in

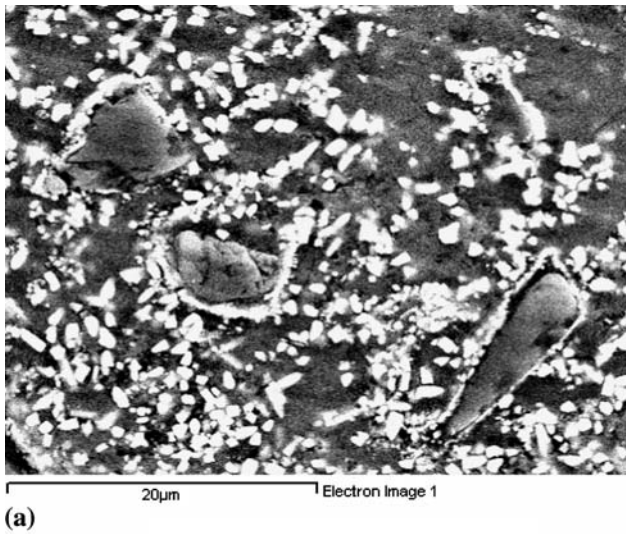

Fig. 10 Element distribution of B area in the weld. (a) Micrograph of the area B; (b) Ti element face distribution; (c) Si element surface distribution

the weld pool also increased. Subsequently, the weld zone formed coarser columnar crystals, as displayed in the SEM micrograph of Fig. 12(c), after the resolidification of the melt.

From the Ti-Al binary phase diagram (Ref 24), it can be anticipated that increasing the content of Ti would lead to the formation of intermetallic compounds like TiAl and Ti_3Al, etc., during the Nd:YAG laser welding. As illustrated by the XRD pattern of the fracture surface of a laser weld joint with the thicker Ti filler (Fig. 13), some brittle intermetallic compounds like TiAl and Ti_3Al had formed. Available literature (Ref 25) shows that TiAl and Ti_3Al are the harmful intermetallic compounds in the weld and tend to decrease the strength of welded joints. Such harmful effect may follow the chemical reaction of 5Ti[All] + 3Al[l] + SiC[s] $\rightarrow$ TiC[s] + Si[Al [l]] + Al[l] + (TiAl + Ti_3Al). Hence, too much thickness of the Ti filler led to (i) the appearance of the large block of columnar crystals in the microstructure (Fig. 14) and (ii) the newly formed reinforcement TiC to be replaced by the melted/re-solidified Ti and subsequently only the melted/re-solidified Ti existed in the weld. Results (Fig. 3, 9, and 11) indicate that there existed an optimal thickness of Ti filler in the individually set parameters in the Nd:YAG laser welding of SiC_p/AlSi7Mg. With the optimal thickness of Ti filler, the initial SiC particles distributed in the AMC would offer a highly dense nucleus area for the in situ TiC nucleation. This would effectively suppress the formation of intermetallic compounds like TiAl and Ti_3Al in the weld. Ultimately this created favorable conditions to provide relatively superior strength to the welded joint compared to conventional laser welding.

3.4 TEM of the Interface Between In Situ Formed TiC and Matrix

The interface between in situ formed TiC and the matrix was analyzed by the TEM micrograph displayed in Fig. 15. It shows a clear interface between the newly formed TiC and the matrix. This suggested the occurrence of prominent in situ reaction to integrate the reinforcement particle with matrix (cf. Fig. 6 and 15), and the high probability of successfully transferring load from the matrix to TiC and vice versa. It also gives indication that the AMC SiC_p/AlSi7Mg would be welded satisfactorily by Nd:YAG laser.

4. Conclusion

Titanium as a filler metal in Nd:YAG laser welding of SiC_p/AlSi7Mg provided beneficial in situ reinforcement effect. Simultaneously, the newly formed reinforcement TiC particles distribute uniformly in the weld that assisted AMC welding. Moreover, Al_4C_3 formation was effectively restrained in the Nd:YAG laser welding of SiC_p/AlSi7Mg with Ti filler.

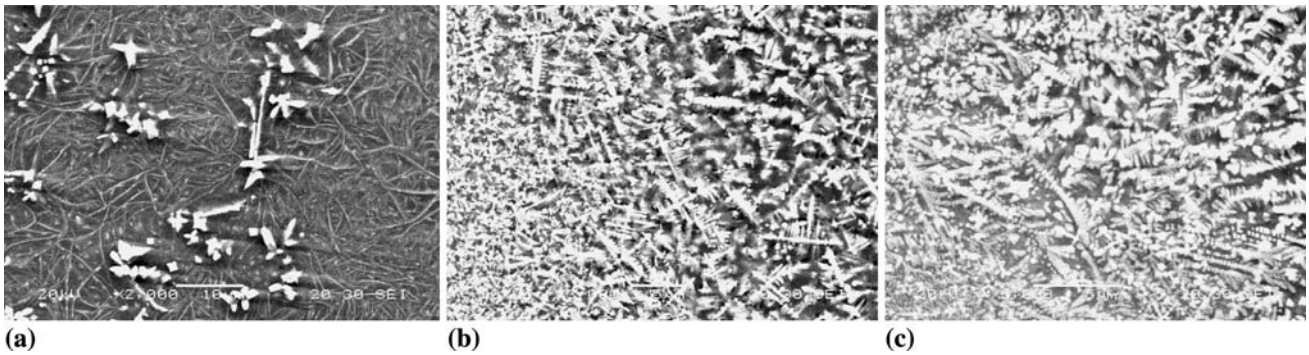

Fig. 11 Microstructures of welded joints with various thicknesses of Ti filler (in area A). (a) δ = 0.15 mm; (b) δ = 0.45 mm; (c) δ = 0.60 mm

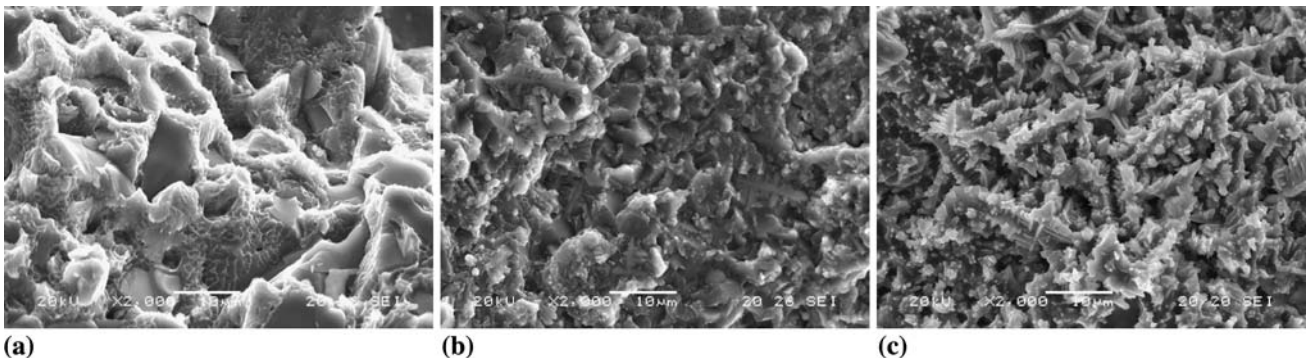

Fig. 12 Fractographs of welded joints with various thicknesses of Ti filler (in area A). (a) δ = 0.15 mm; (b) δ = 0.45 mm; (c) δ = 0.60 mm

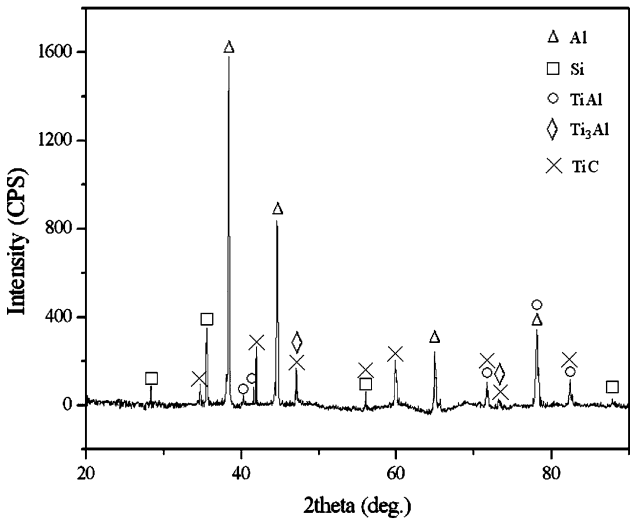

Fig. 13 XRD pattern of fracture surface (δ = 0.6 mm)

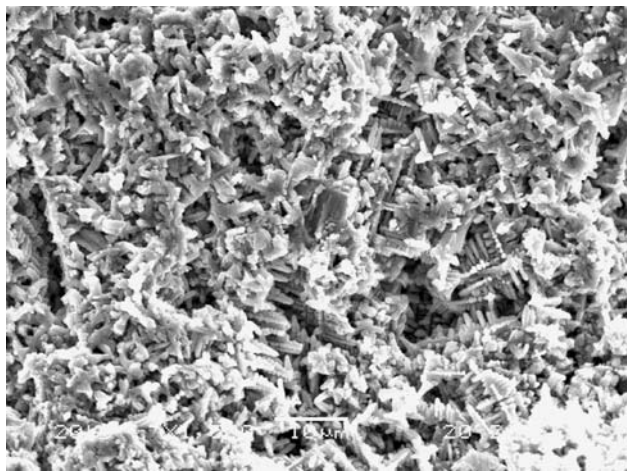

Fig. 14 Columnar crystals in the laser weld with 0.6 mm thick Ti filler

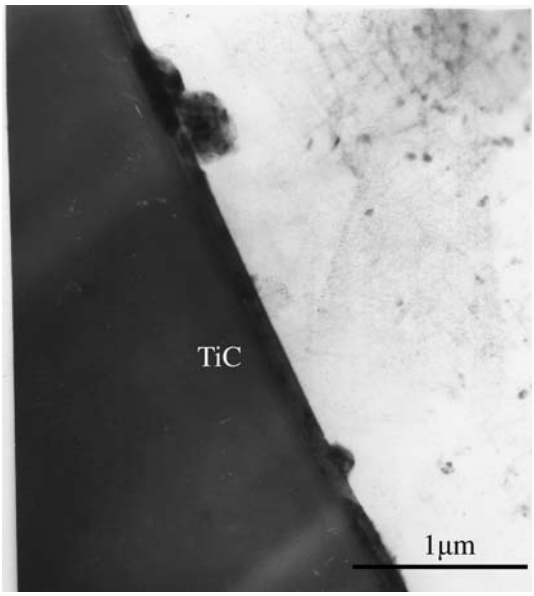

Fig. 15 TEM of interface between in situ TiC reinforcement and the matrix for laser welding with 0.3 mm thick Ti filler

Acknowledgment

The work described in this paper was supported by a Strategic Research Grant (SRG) from City University of Hong Kong (Grant No.: CityUHK 7001978).

References

1. S.V. Nair, J.K. Tien, and R.C. Bates, SiC-Reinforced Aluminum Metal Matrix Composites, *Int. Met. Rev.*, 1985, **30**(6), p 275–290
2. M. Gupta and T.S. Srivatsan, Interrelationship Between Matrix Microhardness and Ultimate Tensile Strength of Discontinuous Particulate-Reinforced Aluminum Alloy, *Mater. Lett.*, 2001, **51**(10), p 255–261
3. Y.L. Shen and N. Chawla, On the Correlation Between Hardness and Tensile Strength in Particle Reinforced Metal Matrix Composites, *Mater. Sci. Eng. A*, 2001, **297**, p 44–47
4. J.M. Gomez de Salazar and M.I. Barrena, Dissimilar Fusion Welding of AA7020/MMC Reinforced with Al_2O_3 Particles: Microstructure and Mechanical Properties, *Mater. Sci. Eng. A*, 2003, **352**, p 162–168
5. D.J. Loyd, Particle-Reinforced Aluminum and Magnesium Matrix Composites, *Int. Mater. Rev.*, 1994, **39**(1), p 1–23
6. T.J. Lienert, E.D. Brandon, and J.C. Lippold, Laser and Electron Beam Welding of SiC_p Reinforced Aluminum A-356 Metal Matrix Composite, *Scr. Metall. Mater.*, 1993, **11**(28), p 1341–1346
7. R.S. Bushby and V.D. Scott, Liquid Phase Bonding of Aluminum and Aluminum/Nicalon Composite Using Interlayers of Cu–Ag Alloy, *Mater. Sci. Technol.*, 1995, **11**, p 643–649
8. J.R. Askew, J.F. Wilde, and T.I. Khan, TLP Bonding of 2124 Aluminum Metal Matrix Composite, *Mater. Sci. Technol.*, 1998, **14**(5), p 920–924
9. K. Ulrich, Tests with regard to the Resistance Spot Welding of Particle-Reinforced Aluminum Matrix Composites, *Weld. Cutt.*, 1999, **51**(1), p 9–12
10. American Welding Society, *Welding Handbook*, American Welding Society, Miami, FL, 1996
11. G. Cam and M. Kocak, Progress in Joining of Advanced Materials, *Int. Mater. Rev.*, 1998, **43**(1), p 1–44
12. J.A. Wert, Microstructures of Friction Stir Weld Joints Between an Aluminum-Base Metal Matrix Composite and a Monolithic Aluminum Alloy, *Scr. Mater.*, 2003, **49**(6), p 607–612
13. G.J. Fernandez and L.E. Murr, Characterization of Tool Wear and Weld Optimization in the Friction Stir Welding of Cast Aluminum A359 + 20% SiC Metal Matrix Composite, *Mater. Charact.*, 2004, **52**(1), p 65–75
14. C.J. Hsu, P.W. Kao, and N.J. Ho, Ultrafine-Grained Al-Al_2Cu Composite Produced In Situ by Friction Stir Processing, *Scr. Mater.*, 2005, **53**(3), p 341–345
15. L.M. Marzoli, A. von Strombeck, J.F. dos Santos, C. Gambaro, and L.M. Volpone, Friction Stir Welding of an AA6061/Al_2O_3/20p Reinforced Alloy, *Compos. Sci. Technol.*, 2006, **66**(2), p 363–371
16. W. Guo, M. Hua, H.W. Law, and J.K.L. Ho, Liquid-Phase Impact Diffusion Welding of SiC_p/6061Al and its Mechanism, *Mater. Sci. Eng. A*, 2008, **490**(1–2), p 427–437
17. W. Guo, M. Hua, and J.K.L. Ho, Study on Liquid-Phase-Impact Diffusion Welding SiC_p/ZL101, *Compos. Sci. Technol.*, 2007, **67**(6), p 1041–1046
18. M. Hua, W. Guo, H.W. Law, and J.K.L. Ho, Half-Transient Liquid Phase Diffusion Welding: An Approach for Diffusion Welding of SiCp/A356 with Cu Interlayer, *Int. J. Adv. Manuf. Technol.*, 2008, **37**(5–6), p 504–512
19. S. Ochiai, *Mechanical Properties of Metallic Composites*, Marcel Dekker, New York, 1994
20. M. Guagliano and M.H. Aliabadi, *Fracture and Damage of Composites*, WIT, Southampton, Boston, 2006
21. D.A. Porter and K.E. Easterling, *Phase Transformations in Metals and Alloys*, 2nd ed., Nelson Thornes, Cheltenham, 2001
22. R. Riedel, *Handbook of Ceramic Hard Materials*, Wiley-VCH, Weinheim, NY, 2000
23. R. Boyer, G. Welsch, and E.W. Collings, *Materials Properties Handbook: Titanium Alloys*, ASM International, Materials Park, OH, 1994
24. J.R. Davis, *ASM Specialty Handbook—Aluminum and Aluminum Alloys*, ASM International, Materials Park, OH, 1993, p 557
25. S. Mall and T. Nicholas, *Titanium Matrix Composites—Mechanical Behavior*, Technomic Pub. Co. Inc., Lancaster, PA, 1998